bioRxiv preprint doi: https://doi.org/10.1101/2023.02.27.530256; this version posted February 27, 2023. The copyright holder for this preprint (which was not certified by peer review) is the author/funder, who has granted bioRxiv a license to display the preprint in perpetuity. It is made available under a CC-BY-ND 4.0 International license.

Drought Recovery Induced Immunity Confers Pathogen Resistance

Natanella Illouz-Eliaz[1,2], Kathryn Lande[3], Jingting Yu[3], Bruce Jow[2], Joseph Swift[1,2], Travis Lee[1,2,4], Tatsuya Nobori[1,2], Rosa Gomez Castanon[2], Joseph R. Nery[2] and Joseph R. Ecker[1,2,4*]

[1]Plant Biology Laboratory, The Salk Institute for Biological Studies, La Jolla, CA 92037, United States
[2]Genomic Analysis Laboratory, The Salk Institute for Biological Studies, La Jolla, CA 92037, United States
[3]The Razavi Newman Integrative Genomics and Bioinformatics Core Facility, The Salk Institution for Biological Studies, La Jolla, CA92037, United States
[4]Howard Hughes Medical Institute, The Salk Institute for Biological Studies, La Jolla, CA92037, United States

* Corresponding author: ecker@salk.edu

bioRxiv preprint doi: https://doi.org/10.1101/2023.02.27.530256; this version posted February 27, 2023. The copyright holder for this preprint (which was not certified by peer review) is the author/funder, who has granted bioRxiv a license to display the preprint in perpetuity. It is made available under a CC-BY-ND 4.0 International license.

Keywords

Plant Stress, Stress Recovery, Plant Immunity, Plant Genomics, Single Cell Transcriptomics.

Summary

Rain-fed plants are subjected to cycles of drought and re-watering. Thus, efficient recovery from drought may be among the key determinants in the success of these plants. We performed a fine-scale time course of bulk RNA sequencing and revealed that transcriptional drought recovery is an active and rapid process involving activating over 3000 recovery-specific genes. We found that upon rehydration, there is a rapid microbial-autonomic induction of the immune system. We termed this response drought recovery-induced immunity (DRII). To reveal the immediate cell-type-specific responses that occur upon recovery we performed a single-nucleus transcriptome analysis of plants recovering from drought and profiled >126,000 transcriptomes. We found that the DRII response manifests in sub-populations of epidermal, trichome, and mesophyll cells immediately following rehydration. Finally, inoculation assays with *Pseudomonas syringae* pv. *tomato* DC3000 demonstrated that DRII increases plant resistance against pathogens. Since rehydration increases microbial proliferation and thus, the risk for infection, the DRII response may be crucial for plant survival in water-fluctuating environments.

bioRxiv preprint doi: https://doi.org/10.1101/2023.02.27.530256; this version posted February 27, 2023. The copyright holder for this preprint (which was not certified by peer review) is the author/funder, who has granted bioRxiv a license to display the preprint in perpetuity. It is made available under a CC-BY-ND 4.0 International license.

Introduction

Drought is one of the most harmful natural disasters, and can cause considerable crop losses (Gupta et al., 2020). Hence, plants' responses to drought have been studied extensively. In most plants, extended periods of water deficit result in reduced growth, premature flowering and flower abortion, fruit abscission, and ultimately decreased yield (Campos et al., 2004; Bruce et al., 2002). The most common drought responses include reduced water potential, cell turgor, stomatal closure (Le-Gall et al., 2015), and inhibition of carbon fixation and primary metabolism (Mao et al., 2015; Qin et al., 2007).

At the molecular level, a substantial number of genes that respond to water deficit have been identified and functionally characterized, including transcription factors (TFs) that regulate drought response (Baldoni et al., 2015; Singh et al., 2015; Mao et al., 2015; Nelson et al., 2007; Shim et al., 2018). In many cases, plants are concurrently exposed to other stresses during drought, such as pathogen attacks. Several studies have shown that the immune system is suppressed during drought, and it was speculated that plants prioritize drought tolerance mechanisms over immunity (Berens et al., 2019; Bostock et al., 2014; Yasuda et al., 2008), resulting in higher susceptibility to pathogens during a drought.

Although drought stress in plants has been a subject of research since the 1920s, what occurs upon rehydration is poorly understood. In nature and agriculture, rain-fed plants experience cycles of drought and rehydration. After dry periods and upon rewatering, crop plants should renew growth as quickly and efficiently as possible to minimize productivity loss. It has long been known that some genes allow plants to overcome fluctuations in water availability. For example, the rapid up-regulation of genes regulating osmolyte accumulation enables water retention by adjusting the cell's osmotic potential (Zhang et al., 1999). A remarkable example of recovery from extreme drought conditions is the resurrection plant. These unique plants can lose over 95 % of their water, enter a long period of anabiosis, and regain full functionality after rehydration (Gechev et al., 2012; Norwood et al., 1999). In addition to the ability to preserve vital cellular components during drying and rehydration, these extreme mechanisms of recovery include the ability to rapidly down-regulate growth-related metabolism in response to water deficiency and the inhibition of dehydration-induced senescence programs. These mechanisms enable rapid reconstitution of photosynthetic capacity after rainfall (Griffiths et al., 2014).

Several more recent studies have recognized the importance of recovery in drought tolerance (Gessler et al., 2020; Hagedorn et al., 2016; Galiano et al., 2011; Brodribb, and Cochard, 2009). Gessler et al. (2020) suggest a broad definition for recovery: "the capacity of individuals and ecosystems to return to the undisturbed state and functioning following a disturbance." Ingrisch and Bahn (2018) propose quantifying resilience by considering both the impact of a disturbance and the recovery rate. In woody plants, drought recovery depends on the severity of the stress: The effects of mild stress are fully and

bioRxiv preprint doi: https://doi.org/10.1101/2023.02.27.530256; this version posted February 27, 2023. The copyright holder for this preprint (which was not certified by peer review) is the author/funder, who has granted bioRxiv a license to display the preprint in perpetuity. It is made available under a CC-BY-ND 4.0 International license.

immediately reversible, while recovery from severe stress is slow and depends on the regrowth capacity of the damaged tissues (Ruehr et al., 2019).

Drought stress in plants induces dramatic changes in the transcriptional landscape (Soma et al., 2021; Bhargava et al., 2013; Shinozaki et al., 2003). Although much is known about the strategies plants have acquired to endure dry periods, few studies have investigated the mechanisms of drought recovery in plants. In *Arabidopsis thaliana* (Arabidopsis) most drought-regulated genes recover to normal expression levels whithin three hours after rehydration (Haung et al., 2008). Studies using DNA microarray and those using chromatin immunoprecipitation (ChIP) assay to explore the nucleosome state during drought and recovery have shown that many drought-inducible genes are repressed by rehydration (Oono et al., 2003; Kim et al., 2012). Previous studies suggest genetic mechanisms of stress memory upon cycles of drought and recovery. (Ding et al., 2012; Kim et al., 2020). Transcriptional memory is associated with two marks that are found in "trainable genes" during recovery: high levels of trimethylated histone H3 Lys4 (H3K4me3) nucleosomes and stalled Ser5P RNA Polymerase II (Pol II) (Ding et al., 2012).

Previous studies have focused on drought-induced genes and thus lack insight into recovery-specific genes that facilitate the recovery response and growth restoration. Kim et al. (2012) found that H3K4me3 modifications to the rehydration-inducible gene, *proline dehydrogenase* (*ProDH*), increase in response to rehydration. However, five hours after rehydration, H3K4me3 enrichment decreases, in accordance with the pattern of RNAP II accumulation in the *ProDH* region. These findings show that the regulation of histone modifications during drought recovery may be one strategy of recovery and regrowth following drought.

Drought recovery is central to any definition of drought resilience, as it reflects the inherent forces that drive a system back to a stable state of function (Gessler et al., 2020). However, it is not yet clear whether plants have specific mechanisms that regulate drought recovery or recovery depends only on drought susceptibility.

Here we study the drought recovery process of *Arabidopsis thaliana*. We traced a fine-scale time course of drought recovery to explore the transcriptomic landscape during recovery. We identified over 3,000 "recovery-specific" genes and validated 296 recovery markers. We found that immune-related genes are upregulated minutes after rehydration in epidermal and mesophyll cell sub-populations, revealing a novel mechanism of preventive immunity activation following moderate drought.

bioRxiv preprint doi: https://doi.org/10.1101/2023.02.27.530256; this version posted February 27, 2023. The copyright holder for this preprint (which was not certified by peer review) is the author/funder, who has granted bioRxiv a license to display the preprint in perpetuity. It is made available under a CC-BY-ND 4.0 International license.

Results

Time-course transcriptome analysis of drought recovery to identify recovery-specific genes.

To measure the transcriptional response to drought recovery, we performed a fine-scale RNA-seq time-course using vermiculite-grown Arabidopsis. Thirty-day-old plants were weighed to determine soil water content (SWC) at saturation (100%) and then transferred to dry trays for drought treatment. When the pots reached 30% SWC, rosettes were collected at time 0 (drought), while other plants were rehydrated for recovery. After the plants were re-watered, rosettes were collected at eight additional recovery time points (Fig. 1 A). At each recovery time point, rosettes were also collected from a well-watered control to control for transcriptional changes created by the output of the circadian clock. We then conducted an intersection analysis of the treatments and time points (Figs. 1 B and S1 A-B). Principal component analysis (PCA) and the number of differentially expressed genes (DEGs) revealed that after six hours, transcription was almost completely recovered (with only 125 DEGs). After 48 hours, it was fully recovered (0 DEGs) (Fig. 1 B-C). We defined two groups of genes in our dataset: drought-responsive and recovery specific. Drought-responsive genes were defined as DE genes under drought- and at any other time point during recovery. Recovery-specific genes were defined as not DE under drought (time 0) but DE in any recovery time points. Based on these definitions, 1248 drought-responsive genes were identified, with 53% (662 genes) also being DE during recovery. More than 1000 (1023=82%) drought-responsive genes were restored to normal levels as fast as 15 min after rehydration. After only six hours of rehydration, 97% of genes return to normal levels (Fig. 1 C). We identified over 3000 recovery-specific genes across all recovery time points (Fig. 1 C, Fig. S1 C-E, and Sup table 1 and 2). These results suggest that drought recovery is an actively controlled process that is more complex than simply restoring the expression of drought-responsive genes to normal levels.

bioRxiv preprint doi: https://doi.org/10.1101/2023.02.27.530256; this version posted February 27, 2023. The copyright holder for this preprint (which was not certified by peer review) is the author/funder, who has granted bioRxiv a license to display the preprint in perpetuity. It is made available under a CC-BY-ND 4.0 International license.

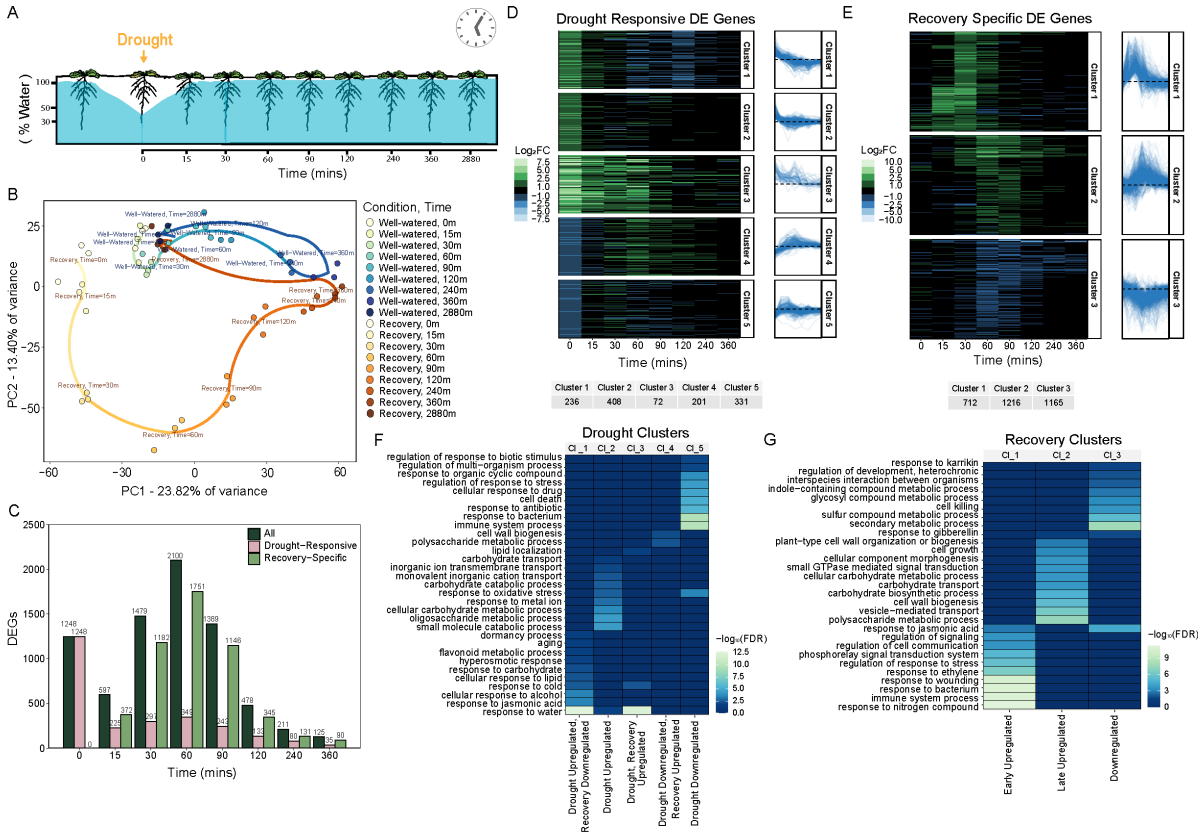


Figure 1. Transcriptional changes during drought recovery. (A) Drought recovery time-course experimental design. **(B)** PCA plot reveals the transcriptional trends underlying drought recover. **(C)** DEGs underlying recovery responses, drought-responsive genes and recovery-specific genes in each time point, treatment vs. well-watered conditions. DEG number was determined as the average of three biological replicated, treatments (drought or recovery) versus well-watered for each time-point. **(D-E)** K-means clustering of **(D)** drought-responsive and **(E)** recovery-specific genes. **(F-G)** GO term enrichment analysis for **(F)** drought-responsive clusters and **(G)** recovery-specific clusters.

Rapid up-regulation of the immune system upon drought recovery.

To unravel the biological processes involved in drought recovery, we used K-means clustering to identify gene expression patterns during the recovery time course. We did this separately for DEGs that were defined as drought-responsive and genes defined as recovery specific. For drought-responsive genes, we identified five distinct expression patterns; (1) drought upregulated, recovery downregulated, (2) drought upregulated, (3) drought and recovery upregulated, (4) drought downregulated and recovery upregulated and (5) drought

bioRxiv preprint doi: https://doi.org/10.1101/2023.02.27.530256; this version posted February 27, 2023. The copyright holder for this preprint (which was not certified by peer review) is the author/funder, who has granted bioRxiv a license to display the preprint in perpetuity. It is made available under a CC-BY-ND 4.0 International license.

downregulated (Fig. 1 D). For recovery-specific genes, we identified three patterns; (1) early upregulated, (2) late upregulated, and (3) downregulated (Fig. 1 E). We examined these drought-responsive and recovery-specific clusters' Gene Ontology (GO) enrichment. We found a striking enrichment in categories associated with plant immunity (GO:0002376) and response to bacteria (GO:0009607) in the recovery-specific clusters. These GO terms were significantly downregulated during drought (Fig. 1 F-G). We also performed the GO term analysis on all DE genes in the data by time-point and direction (Fig S2 A-B). This analysis revealed general stress terms for drought (time 0) and early recovery time points. Nevertheless, our analysis also revealed enrichment in the immune system process (GO:0002376) and response to bacteria (GO:0009607) as fast as 15 minutes after rehydration. This response included known immune receptors such as *FLAGELLIN-SENSITIVE 2* (*FLS2*) and *BRI1-ASSOCIATED RECEPTOR KINASE* (*BAK1*), many immune-related transcription factors (TFs) from the *WRKY DNA-binding protein* (*WRKY*) family and *ARABIDOPSIS THALIANA MITOGEN-ACTIVATED PROTEIN KINASE KINASE 4* (*MKK4*) and *MKK5*, kinases that are involved in innate immunity (Fig. S2 C-J). Out of the ~600 DEGs found 15 mins after rehydration, 10% were genes associated with the immune system process and response to biotic stimuli (Fig. S2 K, Table S3 and S4). It has been previously shown that under abiotic stresses, such as salt and drought stress, plants suppress their immune system via an ABA-triggered immune suppression mechanism (Berens et al., 2019; Audenaert et al., 2002). Indeed, we found ABA-related genes, such as *ABSCISIC ACID RESPONSIVE ELEMENTS-BINDING FACTOR 2 (ABF2/AREB1), ABA-RESPONSIVE ELEMENT BINDING PROTEIN 2 (ABF4/AREB2)* and *ABF3* were highly expressed, and immune-related genes were down-regulated during drought (Fig. S3 A-C).

Recovery from moderate drought induces preventive immune activation.

To understand whether the up-regulation of immunity-related genes was merely the reactivation of the same immune genes that were suppressed during drought, we examined the overlap between the immune genes suppressed by drought and the genes upregulated after 15, 30, and 60 minutes from rehydration (Fig. 2 A-B). In both cases (GO:0002376 and GO:0009607), only 22-23% of the suppressed genes during drought were upregulated in early recovery time points. Thus, most of the rapid recovery upregulated genes were recovery specific, suggesting two separate mechanisms regulating plant immunity under drought stress and recovery. We examined the expression patterns of all genes in each of the immune-related GO terms upon rehydration. This observation reveals a robust but transient up-regulation, starting at 15 minutes after rewatering and returning to baseline after 90-120 minutes (Fig. S3 D-E).

We hypothesized that this transcriptomic immunity exaltation has evolved as an innate response to drought rehydration, regardless of the presence of a preemptive response to imminent microbial spore

bioRxiv preprint doi: https://doi.org/10.1101/2023.02.27.530256; this version posted February 27, 2023. The copyright holder for this preprint (which was not certified by peer review) is the author/funder, who has granted bioRxiv a license to display the preprint in perpetuity. It is made available under a CC-BY-ND 4.0 International license.

germinations and blooms following rewatering. We tested this hypothesis by examining rehydration under axenic conditions, clean from microbial communities. We grew Arabidopsis seedlings on low-water (LW) content agar media (Gonzales et al., 2022) by decreasing the water content (WC) from the media to 50% (moderate osmotic stress) (Fig. S4 A). After 14 days on normal plates, plants were transferred to LW-content plates. After 14 additional days, plants were rehydrated and collected at different time points for RNA-seq analysis. Analysis of known drought marker genes *RESPONSIVE TO DESICCATION 29A (RD29A), RD20*, and *DELTA1-PYRROLINE-5-CARBOXYLATE SYNTHASE 1 (P5CS)* (Msanne et al., 2011; Aubert et al., 2010; Sze´kely et al., 2008) confirmed the moderate drought stress levels (Fig. S 4 B-D). GO term enrichment analysis revealed significant enrichment of the same two immune-related GO terms after 15 minutes in the axenic system (Fig. 2 C). We examined the overlap between 'immune-system process' genes and 'response to bacteria' genes induced after 15 minutes in vermiculite versus on plates. The degree of overlap was 52% for the 'Immune-system process' and 64% for 'response to bacteria' (Fisher's exact test p-value=$4.11*10^{-8}$ and p-value=$1.41*10^{-4}$ respectively; Fig. 2 D-E), suggesting that plants manifest a rapid and transient immune response upon recovery from moderate drought. We termed this response DROUGHT-RECOVERY INDUCED IMMUNITY (DRII).

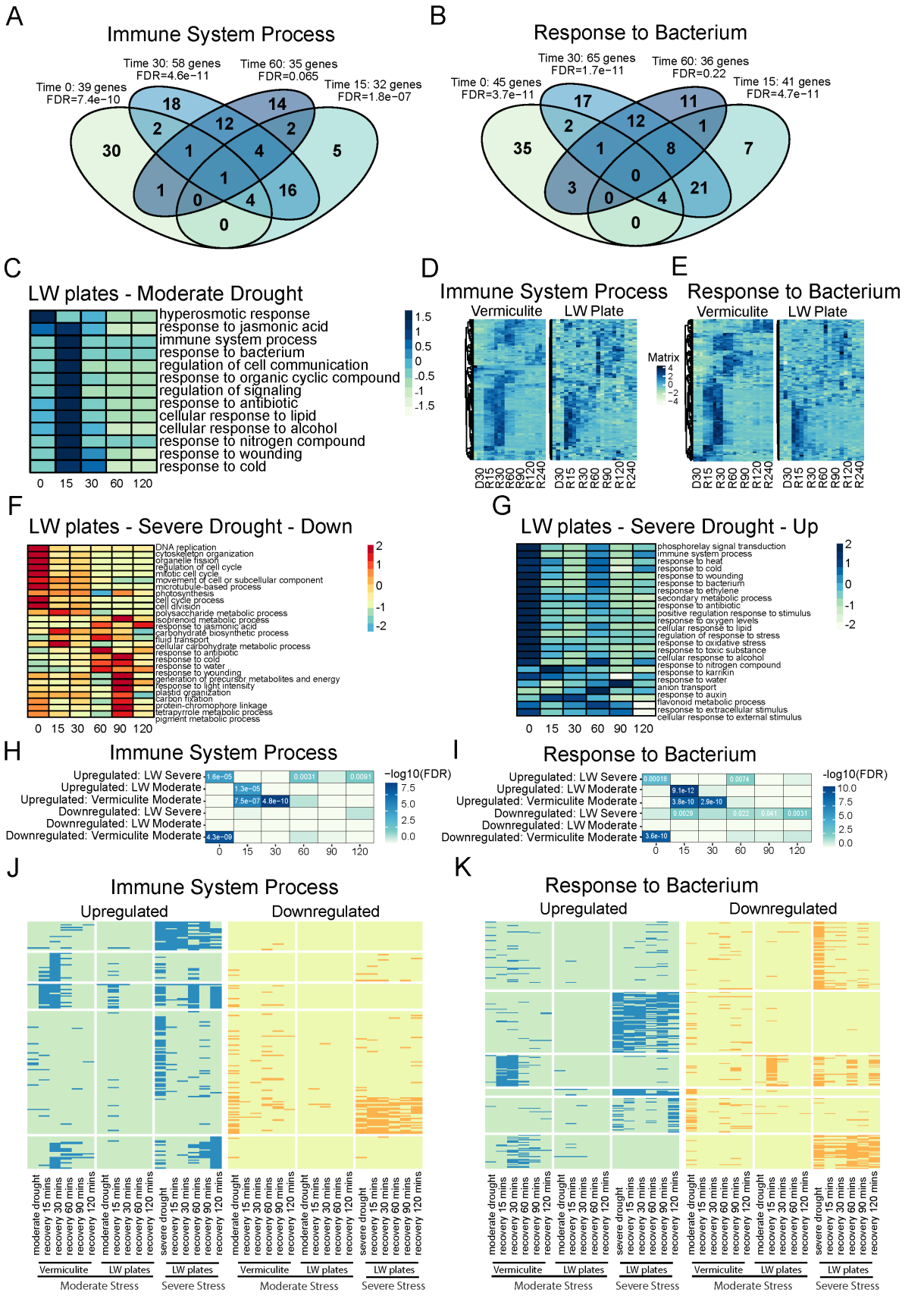
We next explored whether the activation of the immune system by rehydration is consistent under any stress severity. We used the LW plate system to explore recovery from severe stress (i.e. 25% WC) (Fig. S4 A). GO term analysis revealed that biological processes' activation differs from those found under moderate stress. For example, many growth and developmental-related genes were inhibited during severe drought but not during moderate stress. These included cell cycle, DNA replication and photosynthesis genes (Fig. 2 F). Also, the transcriptomic landscape of recovery from severe stress was less plastic than that of plants recovering from moderate stress. Surprisingly, under severe stress, the expression of immune-related genes was up-regulated, contradicting the known drought-induced immune suppression, and different from the results found under moderate stress (Fig. 2 F-G). These findings imply that the DRII response depends on stress severity and is specific to recovery from moderate stress.

To further understand the relationship between the genes that were highly affected by drought and recovered, we examined the significance in enrichment of each experiment and gene expression directionality (up- or downregulated) for both immune-related GO terms to compare overall significance. The results show that these GO terms are upregulated after 15 minutes from rehydration after moderate drought in both vermiculite and LW plates, and down-regulated during drought when stress is severe (Fig. 2 H-I). To see consistency and overlap between the same genes, we generated a binary heatmap that shows all term-annotated DEGs across the three independent experiments, up to two hours of recovery. This analysis establishes that two processes relating to plant immunity take place during drought recovery:

bioRxiv preprint doi: https://doi.org/10.1101/2023.02.27.530256; this version posted February 27, 2023. The copyright holder for this preprint (which was not certified by peer review) is the author/funder, who has granted bioRxiv a license to display the preprint in perpetuity. It is made available under a CC-BY-ND 4.0 International license.

(1) suppressed immune genes return to normal levels after immediate rehydration (as fast as 15 mins), and (2) **a separate but distinct** group of immune-related genes is rapidly upregulated upon rehydration (Fig. 2 J-K).

bioRxiv preprint doi: https://doi.org/10.1101/2023.02.27.530256; this version posted February 27, 2023. The copyright holder for this preprint (which was not certified by peer review) is the author/funder, who has granted bioRxiv a license to display the preprint in perpetuity. It is made available under a CC-BY-ND 4.0 International license.



bioRxiv preprint doi: https://doi.org/10.1101/2023.02.27.530256; this version posted February 27, 2023. The copyright holder for this preprint (which was not certified by peer review) is the author/funder, who has granted bioRxiv a license to display the preprint in perpetuity. It is made available under a CC-BY-ND 4.0 International license.

Figure 2. Recovery from moderate drought induces immune activation. (A-B) Venn diagram exhibiting the overlap between immune genes down-regulated during drought, and genes up-regulated 15, 30 and 60 min after rehydration from **(A)** 'Immune system process' GO term **(B)** 'Response to bacterium' GO term. **(C)** GO term enrichment analysis for genes up-regulated by drought and rehydration in LW sterile plate system. **(D-E)** Heatmaps of genes belonging to **(A)** 'Immune system process' GO term and **(B)** 'Response to bacterium' GO term induced 15 minutes after recovery in vermiculite drought and moderate drought on LW plate system. **(F-G)** GO term enrichment in response to recovery from severe stress for **(F)** down-regulated genes and **(G)** up-regulated genes across time points. **(H-I)** FDR significance of GO term enrichment in independent experiments for **(H)** 'Immune system process' GO term **(I)** 'Response to bacterium' GO terms. **(J-K)** Binary heatmaps, dark versus light show significance or non-significance. **(J)** 'Immune system process' GO term and **(K)** 'Response to bacterium' GO term in vermiculite moderate drought, LW plates moderate drought, and severe drought on LW plate system.

Figure 3. Cell-type specific transcription factor expression during immediate recovery. (A) integrated tSNE representation of >126,000 cells gene expression patterns from four conditions: well-watered, drought recovery 15 minutes and well-watered 15 minutes. **(B)** percentage of cells from each cell type by condition. **(C-F)** tSNE projections of cells for each condition **(C)** well-watered **(D)** drought **(E)** well-watered for 15 minutes and **(F)** drought recovery after 15 minutes. **(G)** Dot plot representing the top cluster marker genes for each cluster and cell type. **(H)** Heatmap showing the expression of DE TFs upon recovery (15 mins) in a cell type-specific manner.

One drought recovery marker gene is known from the literature, *proDH* (Oono et al., 2003). We used the vermiculite dataset to identify marker genes for drought recovery and validated them using the recovery from moderate osmotic stress data (Table S5). We identified a set of 296 early response markers in both datasets that are strongly induced up to 1 hour from rehydration. In our data, *proDH* is upregulated after 30 mins and stays elevated for up to six hours from rehydration. At the same time, the newly identified recovery markers are upregulated after 15-30 mins and are back to control levels after 60-120 mins (Fig S5 A-E).

We used these datasets (Vermiculite, time 15 and 30 min and moderate drought on LW plates, time 15 and 30) in an attempt to identify candidate TFs that may regulate the DRII response. To this end, we identified genes with the top five most enriched DAP-seq (O'Malley et al., 2016) targets against each gene set. We found 12 TFs with significant adjusted p-values that may regulate the DRII response (Table S6).

Cell heterogeneity under moderate drought and immediate recovery.

Plant immune responses are known to be spatially local and cell-type specific (Kawa and Brady, 2022). Thus, we explored if the DRII response is cell-type-specific. To this end, we profiled single-nuclei transcriptomes of vermiculite-grown rosettes under moderate drought and 15 minutes after rehydration. Over 126,000 single-nuclei transcriptomes were obtained from four conditions: well-watered time 0 and 15 mins later, drought (30% SWC) and 15 mins drought-recovery.

First, we examined the expression of characterized drought-induced genes between our control and drought samples, which showed a higher average in drought samples (Table S7). Unsupervised clustering

bioRxiv preprint doi: https://doi.org/10.1101/2023.02.27.530256; this version posted February 27, 2023. The copyright holder for this preprint (which was not certified by peer review) is the author/funder, who has granted bioRxiv a license to display the preprint in perpetuity. It is made available under a CC-BY-ND 4.0 International license.

identified 19 distinct cell clusters (Fig. S6; tSNE and Fig. S7; UMAP). To assign cell identity to the clusters, we examined the specificity of transcripts of known marker genes (Fig. S8, table S9). We annotated the 19 clusters based on literature known marker genes and used TAIR (www.arabidopsis.org/) and ePlant BAR browser (bar.utoronto.ca/eplant/) to identify cell types based on top cluster markers. Plotting the transcriptomes from the four treatments in two dimensions using t-distributed stochastic neighbor embedding (tSNE) revealed an overlapping distribution of cell types (Fig. S6). The 19 clusters covered the major rosette cell types but also included a stress-related cluster (Fig. S6 A; cluster 19). The top cluster marker genes were mainly associated with stress (response to ABA) and defense genes. Based on the annotations of these 19 clusters, we generated a top-level tSNE by cell type, with 9 distinct rosette cell populations (Fig. 3 A). Similar proportions of cell types were found in all four treatments (Fig. 3 B). To study the heterogeneity within cell types, we subclustered each top-level cell type. Most sub-clusters consisted of the top-level cluster annotations; however, some sub-clusters were annotated as others, e.g., Epidermal cells now revealed some sub-cluster being guard cells (Fig. 4 A-B and I-J, Fig. S9). Based on annotations of sub-clusters, we revised the cell type top-level tSNE for further analysis (Table S10).

Since there is a rapid transcriptional response upon drought recovery, we searched for TFs that may account for this transcriptional reprogramming. We overlapped the list of DEGs upon recovery with a list of Arabidopsis TFs and filtered with FDR<0.05 and |average FC|>1.5, and found 52 up- and 7 down-regulated genes in 15 minutes from recovery. Some of these TFs are upregulated in a recovery-specific manner but also in a cell-type-specific manner. For example, in this list, there are members of the *WRKY* (*WRKY41, 75, 53*) TF family induced by recovery, specifically in vascular cells, while *WRKY8* is highly induced in trichomes upon recovery (Fig. 3 H).

bioRxiv preprint doi: https://doi.org/10.1101/2023.02.27.530256; this version posted February 27, 2023. The copyright holder for this preprint (which was not certified by peer review) is the author/funder, who has granted bioRxiv a license to display the preprint in perpetuity. It is made available under a CC-BY-ND 4.0 International license.

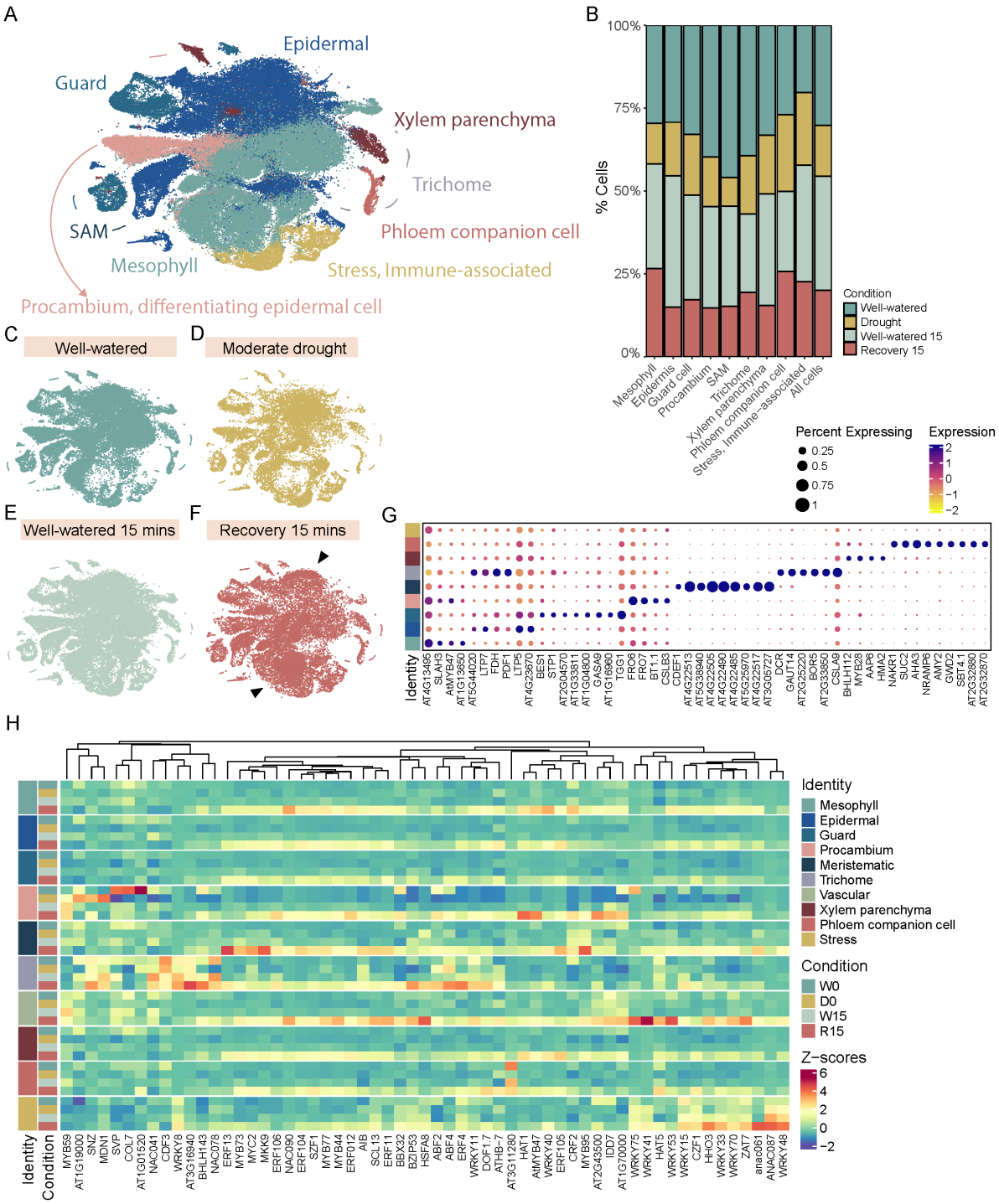


Figure 3. Cell-type specific transcription factor expression during immediate recovery. (A) integrated tSNE representation of >126,000 cells gene expression patterns from four conditions: well-watered, drought recovery 15 minutes and well-watered 15 minutes. **(B)** percentage of cells from each cell type by condition. **(C-F)** tSNE projections of cells for each condition **(C)** well-watered **(D)** drought **(E)** well-watered for 15 minutes and **(F)** drought recovery after 15 minutes. **(G)** Dot plot representing the top cluster marker genes for each cluster and cell type. **(H)** Heatmap showing the expression of DE TFs upon recovery (15 mins) in a cell type-specific manner.

bioRxiv preprint doi: https://doi.org/10.1101/2023.02.27.530256; this version posted February 27, 2023. The copyright holder for this preprint (which was not certified by peer review) is the author/funder, who has granted bioRxiv a license to display the preprint in perpetuity. It is made available under a CC-BY-ND 4.0 International license.

Sub-populations of epidermal, trichome, and mesophyll cells show rapid immune activation upon rehydration.

In contrast with the top-level clustering, the sub-clustering also revealed differences in cell sub-populations enriched during drought or immediately after recovery (Fig. 4 C and J, Fig. S8). Since our recovery time point was just 15 minutes after rehydration, we assume this enrichment uncovers cells that undergo rapid transcriptional reprogramming in response to the rehydration. Some sub-clusters were found mainly in the drought or immediate recovery treatments (Fig. 4 C and J, Fig. S8). For example, sub-clusters 6 and 8 of the epidermal cell sub-clusters, which we annotated as "Epidermal, Stress" and "Epidermal, Trichome", respectively, were mainly found in the recovery treatment (Fig. 4 B-C). We then examined the top cluster markers of this specific sub-cluster to understand the unique identity of these sub-populations, differentiating them from similar sub-clusters. This investigation revealed genes involved primarily in defense responses and immunity. In epidermal cells sub-cluster 6, we found several known immune-related genes and some uncharacterized genes with descriptions related to defense and immunity. For example, *NAC90* - regulation of immune system process; *AT5G41740* is a disease resistance protein; *AGP1* - immune system process and regulation of defense response; *AT2G40000* - Involved in basal disease resistance, and more (Fig. 4 E-F). Sub-cluster 8, had top cluster markers that are immune-related and genes involved in growth and cell wall organization (Table S11). Several immune-related genes were identified as top cluster markers here as well, such as *AT1G29660*, which acts upstream to systemic acquired resistance, *CALMODULIN-BINDING PROTEIN 60B* (*CBP60F*) involved in SA biosynthetic processes, *TETRASPANIN8* (*TET8*), *SALT-INDUCIBLE ZINC FINGER 1* (*SZF1*), a CCCH-type zinc finger protein involved in salt stress and immune responses, *AT4G30210* which Encodes NADPH-cytochrome P450 reductase that catalyzes the first oxidative step of the phenylpropanoid general pathway and defends against herbivores and pathogens, and *AT5G52750* related to defense responses.

Mesophyll cells sub-clustering revealed three sub-clusters highly enriched in recovery: sub-cluster 4, 6, and 8 (Fig. 4 J). Examining top cluster marker genes in sub-cluster 4 showed an increase in calcium signaling and immunity. *AT4G34150* is a member of the *CALCIUM-DEPENDENT LIPID-BINDING (CaLB domain)* family; *CALMODULIN-LIKE 12 (CML12*); *TIR-NBS7* is a *TOLL-INTERLEUKIN-RESISTANCE (TIR) domain-containing* protein; *LIPOXYGENASE (LOX4)* is induced by or abiotic stresses and triggers defense response. Mesophyll sub-cluster 6 genes included immune-associated genes such as *BETA GLUCOSIDASE 18 (BGLU18*) and *AT1G52040*, and top markers were related to JA response. For example, *JASMONATE-ZIM-DOMAIN PROTEIN 9 (JAZ9), JASMONATE RESPONSIVE 1 (JR1), JASMONIC ACID RESPONSIVE 3 (JR3), AT1G61120*, and *PLASTID ENVELOPE ION CHANNELS 1 (PEC1*). Mesophyll sub-cluster 8 showed similar patterns, having several genes related to calcium signaling

bioRxiv preprint doi: https://doi.org/10.1101/2023.02.27.530256; this version posted February 27, 2023. The copyright holder for this preprint (which was not certified by peer review) is the author/funder, who has granted bioRxiv a license to display the preprint in perpetuity. It is made available under a CC-BY-ND 4.0 International license.

and defense as top markers. We performed a GO enrichment analysis on sub-clusters found enriched in recovery samples. Indeed, all sub-clusters enriched in recovery samples showed significant enrichment in immune-related GO terms, supporting our examination of individual top cluster marker genes (Fig. 4 D and K). We imposed the same process for the drought-enriched sub-populations in our data, and interestingly, these had enrichment in immune-related GO terms, as well (Fig. 4 D and K). This is in contrast with the immune suppression observed at the bulk level. These data suggest that although plants dampen immunity at the global level during drought, some cells maintain an increased defense state under moderate drought.

bioRxiv preprint doi: https://doi.org/10.1101/2023.02.27.530256; this version posted February 27, 2023. The copyright holder for this preprint (which was not certified by peer review) is the author/funder, who has granted bioRxiv a license to display the preprint in perpetuity. It is made available under a CC-BY-ND 4.0 International license.

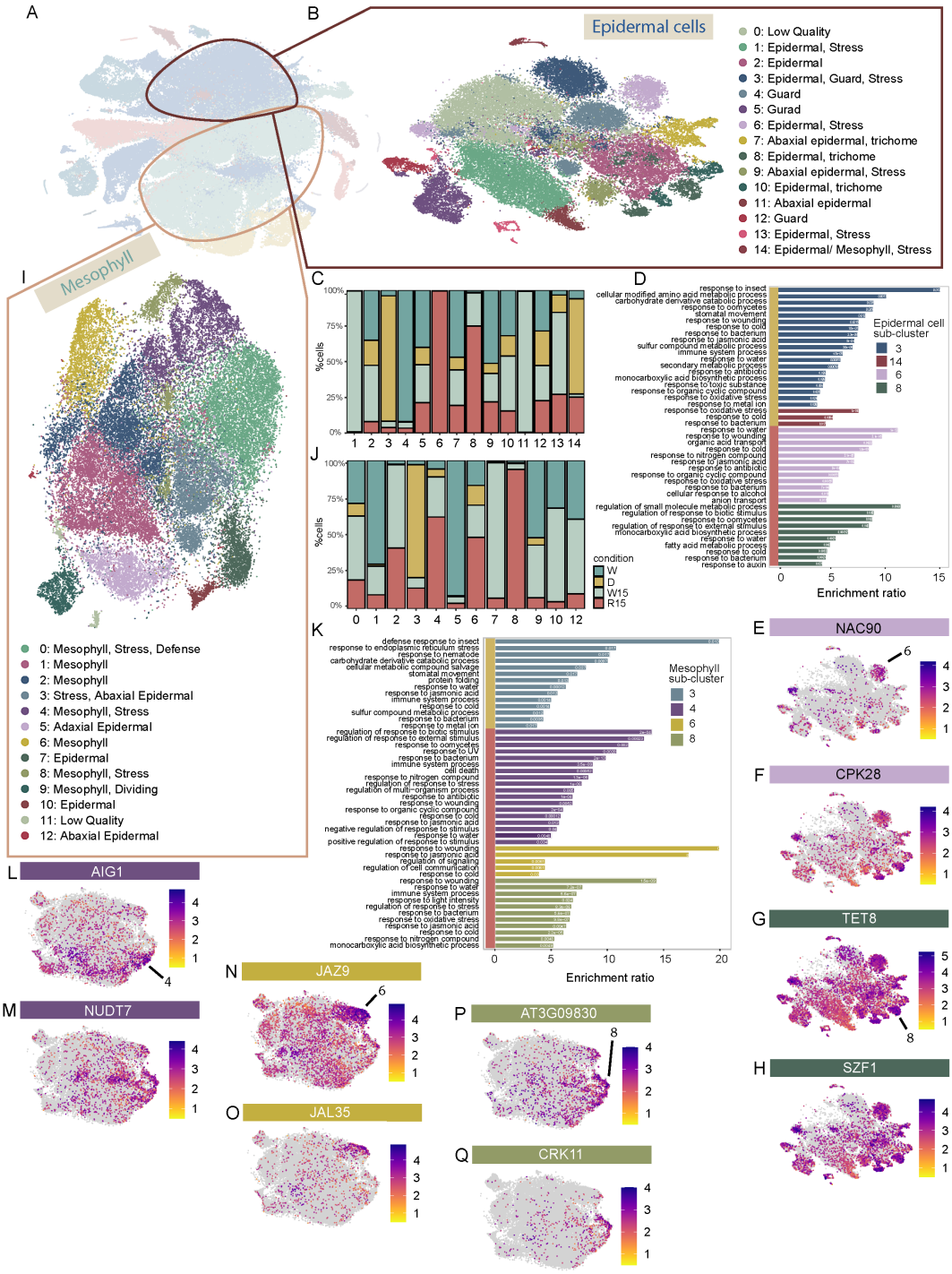
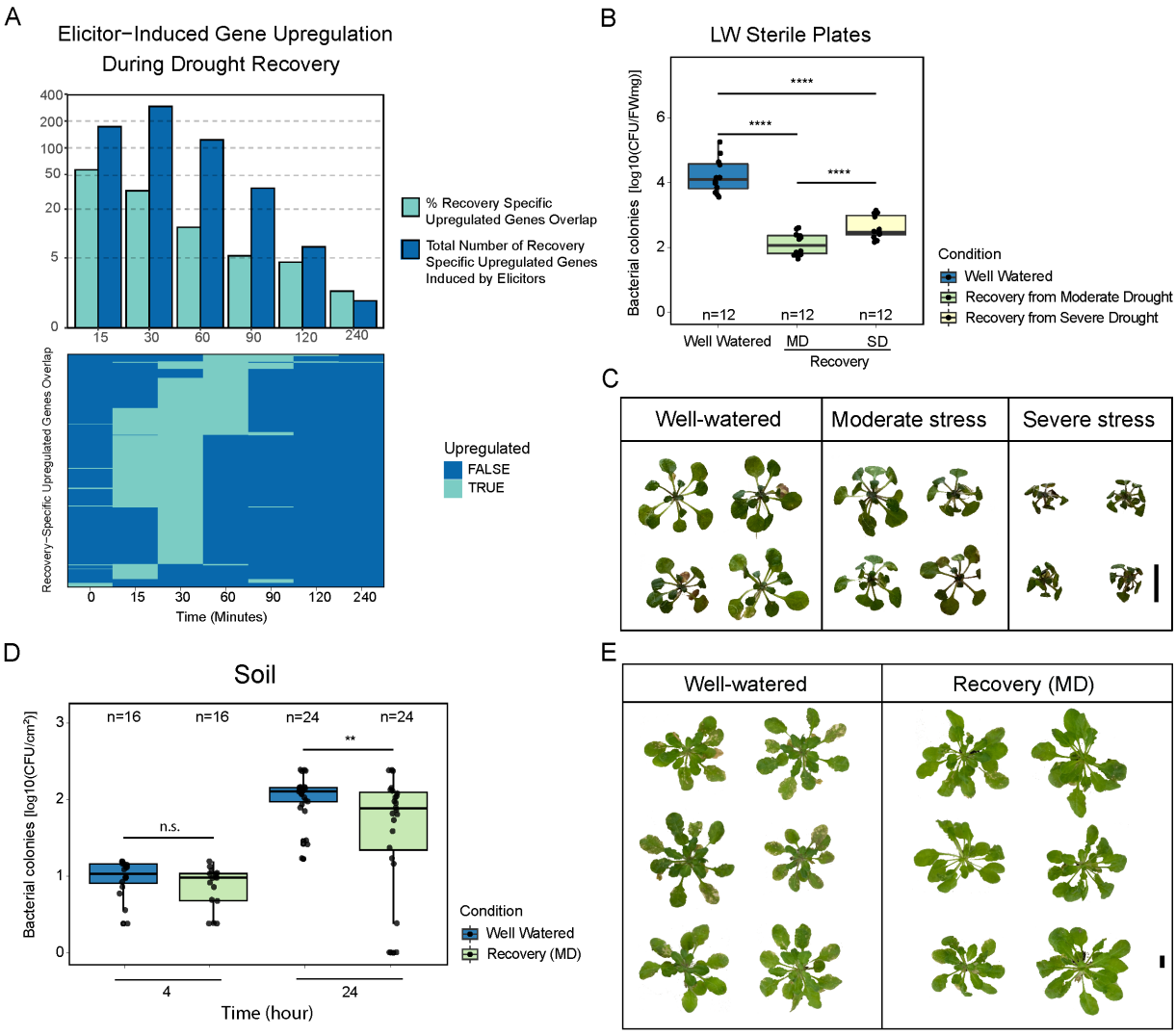


Figure 4. Immune-active cell sub-populations in early recovery. (A) tSNE of major cell types from all four conditions. **(B)** sub-clustering of epidermal cell major cluster. **(C)** percentage of cells in epidermal sub-clusters from each cell type by condition. **(D)** GO term enrichment analysis for drought and recovery enriched sub-clusters. **(E-H)** expression of single genes on the sub-cluster tSNE of **(E-F)** top marker genes in sub-cluster 6 **(G-H)** top marker genes for sub-cluster 8. **(I)** sub-clustering of mesophyll cell major cluster. **(J)** percentage of cells in mesophyll sub-clusters from each cell type by condition. **(K)** GO term enrichment analysis for drought and recovery enriched sub-clusters. **(L-Q)** expression of single genes on the sub-cluster tSNE of **(L-M)** top marker genes in sub-cluster 4 **(N-O)** top marker genes for sub-cluster 6 and **(P-Q)** top marker genes for sub-cluster 8.

bioRxiv preprint doi: https://doi.org/10.1101/2023.02.27.530256; this version posted February 27, 2023. The copyright holder for this preprint (which was not certified by peer review) is the author/funder, who has granted bioRxiv a license to display the preprint in perpetuity. It is made available under a CC-BY-ND 4.0 International license.

Recovery-induced immunity confers pathogen resistance.

Bjornson et al. (2021) performed a transcriptomic analysis in a fine-scale time series to study rapid signaling transcriptional outputs induced by well-characterized patterns of pattern-triggered-immunity (PTI) in Arabidopsis. They show that the transcriptional responses to diverse microbial- or plant-derived molecular patterns are highly conserved. We used this dataset to overlap with our bulk time course of up to two hours to see how the drought recovery transcriptional response correlates to the true response to biotic elicitors. The results showed that after 15 minutes of rehydration, over 50% of recovery-specific genes upregulated in our dataset, overlap with the core response to elicitors from the Bjornson (2021) dataset. The two datasets show a rapid and robust peak of expression that gradually decreased (Fig. 5 A).



bioRxiv preprint doi: https://doi.org/10.1101/2023.02.27.530256; this version posted February 27, 2023. The copyright holder for this preprint (which was not certified by peer review) is the author/funder, who has granted bioRxiv a license to display the preprint in perpetuity. It is made available under a CC-BY-ND 4.0 International license.

Figure 5. Recovery from drought stress enhanced pathogen resistance. (A) Overlap of bulk RNA-seq recovery specific up-regulated genes and Bjornson et al., (2021) genes up-regulated by different biotic elicitors. **(B)** plants grown on LW sterile plates after submergence in *Pto* DC3000 (OD_{600}=0.005) or mock. Bacterial growth was measured at 2 days post-inoculation. (ns = P > 0.05, * = P ≤ 0.05, ** = P ≤ 0.01, *** = P ≤ 0.001, **** = P ≤ 0.0001, we merged two independent experiments, total n=12 per treatment. Significance values for log10(CFU) on the plates were calculated with a two-way ANOVA of treatment and batch followed by a Tukey test. P-values are FDR-corrected) **(C)** Representative plants images four days post-inoculation. **(D)** Soil-grown plants spraying or mock after *Pto* DC3000 (OD600=0.05). Bacterial growth was measured 4 hours and 24 hours post-inoculation. (ns = P > 0.05, * = P ≤ 0.05, ** = P ≤ 0.01, *** = P ≤ 0.001, **** = P ≤ 0.0001, two-way student's t-test) **(E)** representative plants images 14 days post-inoculation.

We examined if short-term recovery from moderate drought and the activation of DRII genes promotes pathogen resistance. To this end, we used the sterile LW plate system and examined recovery from moderate and severe stress as described above. All treated plants (well-watered and drought-treated) were rehydrated for 90 mins before infection with *Pseudomonas syringae* pv. *tomato* DC3000 *(Pto* DC3000*)* by submerging plants in the bacterial suspension. After 48 hours following infection, whole rosettes were collected, weighed, and used to determine bacterial growth. Recovered plants showed a significantly reduced number of bacterial colonies normalized to plant fresh weight. Interestingly, recovery from moderate stress suppressed bacterial growth better than recovery from severe stress (Fig. 5 B-C). These results suggest that recovery from moderate drought enhances plants' defense against *Pto* DC3000. To further validate these results, we grew plants on soil for 30 days under short-day conditions (LD8:16). Control plants were irrigated throughout the experiment, and drought-treated plants were transferred to dry trays and dehydrated for one week (~30% SWC). We rehydrated drought-treated plants for 90 mins and sprayed leaves of control and recovered plants with *Pto* DC3000. Leaf discs were collected from each treatment 4 and 24 hours after inoculation, surface sterilized, and the bacterial load was measured. Samples taken 4 hours after inoculation exhibited a similar bacterial load to that found in control leaves, suggesting that a similar number of bacteria entered the leaves in both well-watered and drought-recovery plants through stomata. However, 48 hours after inoculation, we found a significant decrease in bacterial colonies compared to that found in well-watered plants, suggesting increased resistance to *Pto* DC3000 specific to rehydrated plants (Fig 5 D-E).

Discussion

As large regions on earth gradually dry, drought has become one of the most pressing threats to food security. Thus, plant drought response and the molecular and physiological mechanisms of drought tolerance have been extensively studied over the past decades. Plants encounter, cycles of drought and rehydration in the natural environment and rainfed agriculture. Nevertheless, the molecular mechanisms of plant recovery from drought have been largely overlooked. Here, by separating recovery-specific genes from drought-responsive genes, we were able to parse out the transcriptional response that regulates the

bioRxiv preprint doi: https://doi.org/10.1101/2023.02.27.530256; this version posted February 27, 2023. The copyright holder for this preprint (which was not certified by peer review) is the author/funder, who has granted bioRxiv a license to display the preprint in perpetuity. It is made available under a CC-BY-ND 4.0 International license.

recovery process. The transcriptome recovery process was fast. After 7-10 days without irrigation (when conditions reached 30% SWC), within only six hours from rehydration, the transcriptome was nearly identical to that of plants that did not encounter drought. Within 15 minutes, 82% of the drought-responsive genes restored normal expression levels. These findings may point to the process of recovery having been highly optimized/selected for, to enable rapid repair of gene regulation and, subsequently, rapid renewal of normal development and growth.

In an evolutionarily conserved mechanism, ABA mediates abiotic stress tolerance and suppresses signaling of the biotic stress-related phytohormone salicylic acid (SA). Consequently, plant immunity is decreased during abiotic stresses such as drought and salt (Yasuda et al., 2008). Allocating resources and balancing the trade-offs between biotic and abiotic stress is vital for plant survival and prosperity. Shoot pathogens enter the plant mainly through stomatal pores. Under water-limited conditions, stomata are closed, and the environment is typically less humid, making conditions difficult for pathogens to attack plants successfully. Recently it was shown that beneficial bacteria could improve plant performance under drought stress (Lau and Lennon, 2012). This may also be a cause for adapting the suppressing of the immune system under drought, enabling beneficial bacteria to surround the plant. Our findings propose that the DRII response confers resistance against pathogens, suggesting that this fast transcriptional response to rehydration may have evolved to protect plants against the risk of rehydration-induced bacterial activity between drought periods when plant immune system is suppressed. It was previously shown that plant immunity could be induced sporadically in the absence of pathogenic threat, a process controlled by the circadian clock and driven by daily oscillations in humidity (Mwimba et al., 2018; Wang et al., 2011; Zhou et al., 2015). Such responses allow plants to prepare for the potential increased risk of infection at the time when microbes are anticipated to be most infectious. Rain is a major cause of devastating plant diseases, as fungal spores and bacteria are spread through rain-dispersed aerosols or ballistic particles splashed from neighboring infected plants. Natural raindrops contain bacteria, including plant pathogens such as *Pseudomonas syringae* (Prasanth et al., 2015), *Xanthomonas campestris*, and *Pantoea ananatis* (Schwartz et al., 2003). Similarly, raindrops contain fungi such as *Rhizopus* sp., *Alternaria* sp., *Botrytis cinerea*, *Fusarium* sp., and *Cladosporium* sp. (Palmero et al., 2011). In addition, rain promotes stomatal opening, which facilitates pathogen entry into leaf tissues (Schwartz et al., 2003; Palmero et al., 2011). High humidity, which is usually associated with rain, enhances the virulence of bacterial pathogens (Xin et al., 2016). A recent paper provided evidence for one of the ways plants respond to rain. They showed that trichomes function as mechanosensory cells that support an effective immune response against pathogens (Matsumura et al., 2022). Rehydration following drought promotes pathogens' arise and stomatal opening, and when these come together with the drought-suppressed immune system, it makes plants vulnerable to

bioRxiv preprint doi: https://doi.org/10.1101/2023.02.27.530256; this version posted February 27, 2023. The copyright holder for this preprint (which was not certified by peer review) is the author/funder, who has granted bioRxiv a license to display the preprint in perpetuity. It is made available under a CC-BY-ND 4.0 International license.

pathogen attack. Thus, rapid up-regulation of immune genes may be crucial for plant survival in water-fluctuating environments.

Plants have different strategies for recovering from moderate and severe drought stress. Interestingly, recovering from moderate drought stress appears to have a "stimulating stress" effect. In rats and humans, moderate and transient stress can lead to a stimulatory effect. In contrast, chronic stress suppresses, rather than stimulates, the immune system, increasing the risk for infectious diseases (Sapolsky, R.M., 2000). The immune system is suppressed in plants under moderate drought stress (Berens et al., 2019). However, according to our data, plants' gene expression under severe drought/ osmotic stress suggests an active immune response. However, while recovery from moderate stress leads to increased immunity resulting in increased pathogen resistance, recovery from severe stress may differ.

Plants, unlike humans, rely solely on the innate immune system. In addition, plants do not have specialized immune cells; in theory, all cells can perceive pathogenic threats and respond. Recently, several publications unveiled various examples of local and cell-type-specific immune responses (Kawa and Brady, 2022; Emonet et al., 2021; Froschel et al., 2021; Rich-Griffin et al., 2020; Zhou et al., 2020). However, these examples were shown in roots. Different cell types present a unique set of molecular signatures, and root responses to environmental signals were shown to have a high level of cell-type specificity (Iyer-Pascuzzi et al., 2011). Zhou et al. (2020) showed that microbe-associated molecular patterns (MAMPs) responses in the root are confined to the root cap and elongation zone while absent from the differentiated zone. They found a strong localized immune response upon cellular damage alongside a pathogenic attack (induced by *flg22*). The damaged cells cause increased expression of PRRs in adjacent cells.

Our results suggest partial cell-type specific immune responses during drought and recovery from drought. Specifically, our single-nuclei data imply that upon drought and early recovery, there are cell-types in which their sub-populations shift to unique cell states specific to these environmental conditions. These sub-populations exhibited the expression of immune genes. For example, we hypothesize that the observed immune response in sub-clusters of mesophyll cells has evolved as a selective defense mechanism during times of high risk, such as rehydration after drought. This rapid response could provide efficient defense against a pathogenic attack, but on the other hand, allow normal functionality of other mesophyll cells that are important for photosynthesis which is suppressed under drought (Bhargava et al., 2013; Rizhsky et al., 2002). Individual root cell types exhibit quantitative differences in the transcriptional output upon flg22 treatment, suggesting a range of sensitivity to recognition by the FLS2 receptor, from the epidermis (extremely sensitive) to the vasculature (almost no response) (Emonet et al., 2021). Cell-type specificity was also observed in some species' responses to fungal MAMPs, where only atrichoblasts and

bioRxiv preprint doi: https://doi.org/10.1101/2023.02.27.530256; this version posted February 27, 2023. The copyright holder for this preprint (which was not certified by peer review) is the author/funder, who has granted bioRxiv a license to display the preprint in perpetuity. It is made available under a CC-BY-ND 4.0 International license.

not trichoblasts initiate the calcium oscillations required for the establishment of symbiosis (Sun et al., 2015). In the presence of pathogenic bacteria, defense responses are initiated only when MAMP detection is accompanied by likely mechanical damage, each occurring in different cell types (Zhou et al., 2020). For example, cell death induced by pathogenic bacteria in the differentiated epidermis activates transcriptional responses to MAMPs in neighboring cortex cells (Zhou et al., 2020). Together, these highly localized immune responses, restricted to individual cell types, allow the root to accommodate innocuous (non-harmful and non-beneficial) bacteria and to prevent inhibition of root growth by excessive defense activity (Kawa and Brady, 2022).

Interestingly in mesophyll sub-cluster 4, one of the top marker genes we found was *Nudix Hydrolase (NUDT7)*, which negatively regulates EDS1-conditioned plant defense and programmed cell death (PCD) (Bartsch et al., 2006). In mesophyll sub-cluster 8, we identified the gene expression involved in the negative regulation of defense, *AT3G52400* syntaxin. This protein is involved in negatively regulating PCD, SA, and JA signaling pathways (Zhang et al., 2007). These findings are in contrast to the increased immunity upon recovery. Since this innate immune response is assumed to be a preventive response regardless of the presence of pathogenic bacteria, there may be a mechanism for avoiding an auto-immune response that imposes cell death in case of non-infection.

The extensive research on how plants respond to drought yielded many discoveries. Yet, the translation of these findings to the development of drought-tolerant crops is minimal (Dalal et al., 2017). The gap between the large research efforts and the actual translation into drought-tolerant crops is primarily due to the trade-off between drought tolerance and growth. The inhibition of plant biomass and yield may be an intrinsic consequence of drought-tolerance acquisition. Improving plant production in the face of global warming and climate change has focused mainly on improving the robustness and efficiency of the drought response, due to an assumption that what happens upon rehydration is simply reversing drought effects. Our findings demonstrate the activity of recovery-specific molecular mechanisms that are vital for successful recovery. We here propose an additional approach to improve plant performance under fluctuating water availability by maintaining a robust drought response and improving recovery abilities. We hypothesize that these recovery-specific genetic components drive rapid recovery upon rehydration. These genetic components may be harnessed to improve crop performance under cycles of drought and rehydration while minimizing yield loss.

bioRxiv preprint doi: https://doi.org/10.1101/2023.02.27.530256; this version posted February 27, 2023. The copyright holder for this preprint (which was not certified by peer review) is the author/funder, who has granted bioRxiv a license to display the preprint in perpetuity. It is made available under a CC-BY-ND 4.0 International license.

Methods

Plant materials and growth conditions

Arabidopsis thaliana Columbia-0 (Col-0) background was used throughout this study. Col-0 seeds were sterilized with chlorine fumes generated by mixing 100 ml bleach and 4 ml hydrochloric acid (HCl 1M). Sterilized seeds were sown on ¾ Linsmaier & Skoog with buffer (LS) media per liter 2% agar, stratified at 4 °C for three days, and grown in short-day conditions (8h light: 16h dark) at 22 °C with a light intensity of ~110–130 μmol m^{-2} s^{-1}. For drought treatments, seedlings were transferred to vermiculite pots two weeks after germination on plants, with 6 seedlings per pot. Tray size was 27.79 cm width, 54.46 cm length, and 6.2 cm depth. Each tray fits 12 pots. Vermiculite was saturated with ¾ LS liquid media before the seedling transfer, 2L media per tray. After two days, each tray was watered with 2L ultra-pure water, and this continued for two weeks until the drought treatment started. When plants were 30 days old, each pot was weighed and transferred to a dry tray. The pots in the tray were weighed daily, and relative water content was calculated. The experiment started when the pots reached 30% soil-water content (SWC). Three whole Arabidopsis rosettes per treatment were collected separately as an independent sample. Three samples per treatment were collected alongside a well-watered control at each time point. For sterile low-water agar experiments, plates were prepared based on Gonzales et al., 2022; 100% - 4L DDW, 3 LS bags, 80g agar – 120ml per plate, 50% (moderate stress) - 2L DDW, 3LS bags, 80g agar – 60ml per plate, and 25% (severe stress) - 1L DDW, 3LS bags, 80g agar – 30ml per plate.

Col-0 seeds were sterilized and seeded on plates. Plates were kept in the dark at 4C for three days. After three days, plates were moved to a growth chamber with short-day photoperiod light and 22 °C temperature.

Bacterial infection

Pseudomonas syringae pv. tomato (Pto) DC3000 strains were grown overnight in 10 ml liquid King's B medium containing rifampicin (40 μg/ml) and tetramicin (10 mg/ml) at 28°C for one day. Before adjusting the density, bacterial cells were washed two times with autoclaved water followed by centrifugation at 6,000 rpm for 2 min and re-suspension in water. For bacterial growth assays, well-watered and 90 min recovered plants were inoculated with *Pto* DC3000 (OD600 = 0.005-0.5, depending on experiment and inoculation method). Bacterial titer was assessed as the log10 transformed colony forming units (CFU) per plant weight when collected whole plants and not leaf discs.

bioRxiv preprint doi: https://doi.org/10.1101/2023.02.27.530256; this version posted February 27, 2023. The copyright holder for this preprint (which was not certified by peer review) is the author/funder, who has granted bioRxiv a license to display the preprint in perpetuity. It is made available under a CC-BY-ND 4.0 International license.

RNA extraction, bulk RNA library construction

Total RNA was extracted from three independent biological replicates of each time-point using RNeasy Plant Mini Kits (Cat#79254, Qiagen, CA). Tape Station checked RNA quantity for quality control. Library construction was performed using Illumina Stranded mRNA Prep (Cat# 20040534, Illumina, CA).

Nuclei extraction and single-nuclei library construction

Seedlings were transferred to vermiculite pots two weeks after germination in trays, 6 seedlings per pot. Vermiculite was saturated with ¾ LS liquid media before the seedling transfer, 2L media per tray. After two days each tray was watered with 2L ultra-pure water, and this continued for two weeks until the drought treatment started. When plants were 30 days old, each pot was weighed and transferred to a dry tray. The experiment began when each pot reached 30% SWC. Between 12-18 whole rosettes were collected for each time point * condition sample. We used mortar and pestle to grind the frozen tissue. Powdered tissue was then placed in a nuclei extraction buffer [NEB; 500ul 1M TRIS pH=7.4 (Cat# 15567027, Thermo Fisher Scientific, MA), 150ul 1M $MgCl_2$ (Cat# AM9530G, Fisher Scientific, MA), 100ul 1M NaCl (Cat# AM9760G Fisher Scientific, MA), 50ml nuclease-free water (Cat# AM9937 Thermo Fisher Scientific, MA), 25ul 1M spermine (Cat# 85590-5G, MilliporeSigma, MA), 10ul 1M sperimidine (Cat# S2626-5G, MilliporeSigma, MA), 500ul proteinase inhibitor (PI; Cat# P9599-5ML MilliporeSigma, MA), 250ul BSA (Cat# B2518-100MG, MilliporeSigma, MA), 250ul SUPERase-In (Cat# AM2696, Thermo Fisher Scientific, MA)] and incubated for 10 min. After incubation, tissue was filtered through a 40um filter (Cat# 43-57040-51, pluriSelect, Germany). We then centrifuged at 500 rcf for 5 min at 4°C. Supernatant was aspirated out, and nuclei were resuspended with NEB + 500ul 10% Triton (Cat# 93443-100ML, MilliporeSigma, MA) and no PI. We incubated for 15 min, filtered through a 40um filter and spun at 500 rcf for 5 min. We washed until the pellet was clear. We prepared the density gradient using the Density Buffer [DB; 120 mM Tris-Cl pH=8 (Cat# AM9855G, Fisher Scientific, MA), 150 mM KCl (Cat# AM9640G, Fisher Scientific, MA), 30 mM MgCl2, 35mL H_20 per 50mL] and filter sterilized it. We mixed 5 volumes of Optiprep (Cat# D1556-250ML, MilliporeSigma, MA) and the buffer volume to create a 50% stock. We also made a dilutant stock [400 mM Sucrose, 25 mM KCl, 5 mM $MgCl_2$, 10 mM Tris-Cl pH 8, 28mL H20 per 50mL] that we filter sterilized. A 45% solution was made by mixing 9ml 50% solution and 1ml dilutant, and a 15% solution by combining 1.5ml 50% stock and 3.5ml dilutant. We created a 45% solution and a 15% solution. We gently poured 2ml of the nuclei solution at the top of the density gradient and then spun the tubes at 1,500 rcf for 5 min with no breaks. After the spin, we pipette off nuclei and place them into a 15 ml tube with ~ 6mL of NEB (with no triton or PI). After counting the nuclei, the nuclei suspension was loaded onto microfluidic chips (10X Genomics) with HT-v3.1 chemistry to capture ~20,000 nuclei/sample. Cells were barcoded with a Chromium X Controller (10X Genomics). mRNA was reverse transcribed, and Illumina libraries were constructed for sequencing with reagents from a 3' Gene Expression

bioRxiv preprint doi: https://doi.org/10.1101/2023.02.27.530256; this version posted February 27, 2023. The copyright holder for this preprint (which was not certified by peer review) is the author/funder, who has granted bioRxiv a license to display the preprint in perpetuity. It is made available under a CC-BY-ND 4.0 International license.

HT-v3.1 kit (10X Genomics) according to the manufacturer's instructions. cDNA and final library quality were assessed using Tape-Station High Sensitivity DNA Chip (Agilent, CA).

Each of the single-nuclei samples was processed twice, to get a higher number of single nuclei transcriptomes.

Bulk RNA-sequencing and analysis

Sequencing was performed with a NovaSeq 6000 instrument (Illumina, CA). About 40 million reads were obtained for each sample. Raw reads were processed at the IGC bioinformatics core at Salk. Alignments were performed using OSA4, and mapped to the A. thaliana genome (TAIR 10) using Tophat2 software with default settings. Mapped reads per library were counted using HTSeq software. Differentially expressed genes were quantified in two ways. Firstly, differentially expressed genes were identified using a spline regression model in splineTimeR v1.18.0, which were then sorted into time points using k-means clustering. Differential expression was also quantified at each time point individually using DESeq2 v1.30.0 (Love et al., 2014). For each pairwise comparison, genes with fewer than 32 total raw counts across all samples were discarded before normalization. Genes with an absolute $\log_2$foldchange > 1 and an FDR-corrected p-value ≤ 0.01 were pulled as significant. For functional enrichment, genes were queried for time-specific functional enrichment using over-representation analysis (ORA) in WebGestaltR v0.4.4 (Liao et al., 2019). Differentially expressed genes in each pairwise comparison were queried against the biological process non-redundant ontology, and a significance threshold of FDR-corrected p-value ≤ 0.05 was used.

For motif discovery sequences 1000-1bp upstream of the CDS of differentially expressed genes at each time point were extracted and queried for the enrichment of known motifs from the Plant Cistrome Database (O'Malley et al., 2016) using the MEME Suite v5.0.2 AME function (McLeay and Bailey, 2010). Up- and down-regulated genes were queried separately at each time point, and absolute $\log_2$foldchange was used as a scoring metric for AME.

snRNA-seq analysis

For the snRNA-seq libraries, CellRanger (v.6.0.1) was used to perform sample-demultiplexing, barcode processing, and single-nuclei gene-UMI counting (Zheng et al., 2017). Each experiment's expression matrix was obtained by aligning to the Arabidopsis transcriptome reference (TAIR 10) using CellRanger with default parameters. For initial quality-control filtering, aligned cell and transcript counts from each treatment (well-watered, drought, recovery, 2 replicates each) were processed by Seurat (Version 4.2) (Hao et al., 2021). The data was filtered in the following two ways: (1) Pre-filtering each replicate by removing the low-quality cells containing a high abundance of chloroplast reads (greater than 40% of total transcripts) and mitochondrial reads (greater than 1% of total transcripts) (Table S8). (2) Identifying possible doublet

bioRxiv preprint doi: https://doi.org/10.1101/2023.02.27.530256; this version posted February 27, 2023. The copyright holder for this preprint (which was not certified by peer review) is the author/funder, who has granted bioRxiv a license to display the preprint in perpetuity. It is made available under a CC-BY-ND 4.0 International license.

clusters in integrated data using the method SCDS. SCDS implements two complementary approaches to identify doublets: one is co-expression-based doublet scoring, and the other is binary classification-based doublet scoring. Additionally, they provide a hybrid score by combing these two approaches. SCDS showed relatively high detection accuracy and computational efficiency when benchmarking with other computational methods (Nan Miles, X. and Li, J.J., 2021). We applied the hybrid scores for doublet estimation using R package scds() to identify likely doublet and then calculated the proportion of likely doublets in clusters. We removed clusters with estimated doublets >=40%. All 19 clusters passed the quality control.Expression data of cells passing these thresholds were log normalized with NormalizeData() function, and the top2K variable genes were identified with the FindVariableFeatures() function. Next, data from all conditions were integrated using Seurat's reciprocal PCA (RPCA) and FindIntegrationAnchors() functions to identify integration features and correct for potential batch effects. The integrated data were then scaled with ScaleData() function. Principal component analysis (PCA) was carried out with RunPCA() function, and the top 30 principal components (PCs) were retained. Clusters were identified with the FindClusters() function using the shared nearest neighbor modularity optimization with a clustering resolution set to 0.8. Clusters with only one cell were removed. This method resulted in 19 initial clusters. To further check the quality of remaining cells at the cluster level, we applied the hybrid scores for doublet estimation using R package scds() to identify likely doublet and then calculated the proportion of likely doublets in clusters (Bais and Kostka, 2020). We removed clusters with estimated doublets >=40%. All 19 clusters passed the quality control. Finally, 126,318 cells were distributed in the initial 19 clusters. We identified a median number of 409 genes, and 628 unique molecular identifiers (representing unique transcripts), per nuclei. We detected between 23,550-25,200 genes in each sample consisting of 87%-92% of Arabidopsis protein-coding genes. After determining the initial cell-type identity, clusters annotated with the same cell identity were grouped together, followed by sub-clustering each major cell-type cluster using the same strategy described above. For each cell type, cells were extracted with the Seurat subset() function and were re-integrated by experiments using RPCA. After annotating the sub-clusters, we further identified some clusters with low-quality cells, as the majority of their top sub-cluster markers were chloroplast genes. Thus, cells from low-quality and unannotated sub-clusters were filtered. Finally, sub-clusters annotation was used to refine the identification of main cell types and resulting in 9 main cell types.

Differential gene expression analysis was conducted using Seurat FindMarker() and FindAllmarkers() functions with the default Wilcoxon Rank Sum test. We identified the cluster markers by setting parameter min pct as 0.1 and picked the top15 markers ranking by average $\log_2$FC. These markers were used to determine cell identity. For differential comparisons between conditions, the parameter min pct was set to 0.05 to include more genes that might not be widely detected.

bioRxiv preprint doi: https://doi.org/10.1101/2023.02.27.530256; this version posted February 27, 2023. The copyright holder for this preprint (which was not certified by peer review) is the author/funder, who has granted bioRxiv a license to display the preprint in perpetuity. It is made available under a CC-BY-ND 4.0 International license.

Functional enrichment analysis was carried out by over-representation analysis (ORA) using the top100 markers ranked by average log_2FC. Using the GO biological process as a reference, ORA was performed with WebGestalt (Liao et al., 2019). Pathways with FDR <0.05 were considered significantly enriched and visualized as plots with normalized enrichment scores.

Statistical analysis

bulk RNA-seq data, statistical analysis was performed in R using a mixed linear model function (lmer) from the package lme4 unless otherwise described. Standard errors were calculated from variance and covariance values after model fitting. The Benjamini-Hochberg method was applied for correcting of multiple testing in figures showing all pairwise comparisons of the mean estimates. For bacterial colonies count, merged two independent experiments of plants grown on plates, a total of n=12 per treatment. Significance values for log10(CFU) on the plates were calculated with a two-way ANOVA of treatment and batch followed by a Tukey test. P-values are FDR-corrected. For bacterial colonies count, soil grown plants experiment, significance values for log10(CFU) were calculated with a two-way student's t-test.

Code availability

The code used to analyze both bulk and single-nuclei RNA-Seq data is available at: https://github.com/NatanellaIE/DroughtRecovery.

Acknowledgments

We thank Omri Finkel and Trevor Nolan for critical reading of the manuscript. This research was supported by a Postdoctoral Award No. FI-601-2020 from BARD, The United States - Israel Binational Agricultural Research and Development Fund.

N. I-E is a research fellow at the George E. Hewitt Foundation for Medical Research and an Awardee of the Weizmann Institute of Science – Israel National Postdoctoral Award Program for Advancing Women in Science. J.S is an Open Philanthropy awardee of Life Science Research Foundation, as well as recipient of the Pratt Industries American-Australian Association Scholarship. J.R.E is an Investigator of the Howard Hughes Medical Institute.

Author contributions

Conceptualization – N.I-E

Data curation – N.I-E, R.G-C, B.J

Formal analysis – N.I-E, K.L, J.Y, J.R.N

Funding acquisition - J.E, N.I-E

bioRxiv preprint doi: https://doi.org/10.1101/2023.02.27.530256; this version posted February 27, 2023. The copyright holder for this preprint (which was not certified by peer review) is the author/funder, who has granted bioRxiv a license to display the preprint in perpetuity. It is made available under a CC-BY-ND 4.0 International license.

Investigation - N.I-E, R.G-C

Methodology - N.I-E, T.L, J.S

Project administration - N.I-E

Resources – J.E

Writing – original draft - N.I-E, J.E.

Declaration of interests

The authors declare no competing interests.

Tables

Table S1. Recovery-specific genes.
Table S2. Drought-responsive genes
Table S3. Immune genes up-regulated after 15 minutes of rehydration.
Table S4. 'Response to bacterium' genes up-regulated after 15 minutes of rehydration.
Table S5. Drought early markers validated in LW plates system. (stage 1- up to 1 hour, stage 2-1 hour and up, only from run1)
Table S6. DRII potential regulators
Table S7. Average expression of drought markers in drought sample versus well-watered
Table S8. Single-cell sequencing summary
Table S9. Unsupervised tSNE cluster markers.
Table S10. Revised cell-type level tSNE cluster markers.
Table S11. Epidermal cell sub-cluster top 50 markers.

References

1. Gupta, A., Rico-Medina, A. & Caño-Delgado, A. I. The physiology of plant responses to drought. **368**, 266–269 (2020).

2. Campos, H., Cooper, M., Habben, J. E., Edmeades, G. O. & Schussler, J. R. Improving drought tolerance in maize: A view from industry. *F. Crop. Res.* **90**, 19–34 (2004).

3. Bruce, W. B., Edmeades, G. O. & Barker, T. C. Molecular and physiological approaches to maize improvement for drought tolerance. *J. Exp. Bot.* **53**, 13–25 (2002).

4. Le Gall, H. *et al.* Cell wall metabolism in response to abiotic stress. *Plants* **4**, 112–166 (2015).

5. Mao, H. *et al.* A transposable element in a NAC gene is associated with drought tolerance in maize seedlings. *Nat. Commun.* **6**, 1–7 (2015).

6. Qin, F. *et al.* Regulation and functional analysis of. **50**, 54–69 (2007).

7. Baldoni, E., Genga, A. & Cominelli, E. Plant MYB transcription factors: Their role in drought response mechanisms. *Int. J. Mol. Sci.* **16**, 15811–15851 (2015).

8. Singh, D. & Laxmi, A. Transcriptional regulation of drought response: A tortuous network of transcriptional factors. *Front. Plant Sci.* **6**, 1–11 (2015).

bioRxiv preprint doi: https://doi.org/10.1101/2023.02.27.530256; this version posted February 27, 2023. The copyright holder for this preprint (which was not certified by peer review) is the author/funder, who has granted bioRxiv a license to display the preprint in perpetuity. It is made available under a CC-BY-ND 4.0 International license.

9. Nelson, D. E. *et al.* Plant nuclear factor Y (NF-Y) B subunits confer drought tolerance and lead to improved corn yields on water-limited acres. *Proc. Natl. Acad. Sci. U. S. A.* **104**, 16450–16455 (2007).

10. Shim, J. S. *et al.* Overexpression of OsNAC14 improves drought tolerance in rice. *Front. Plant Sci.* **9**, 1–14 (2018).

11. Berens, M. L. *et al.* Balancing trade-offs between biotic and abiotic stress responses through leaf age-dependent variation in stress hormone cross-talk. *Proc. Natl. Acad. Sci. U. S. A.* **116**, 2364–2373 (2019).

12. Bostock, R. M., Pye, M. F. & Roubtsova, T. V. *Predisposition in plant disease: Exploiting the nexus in abiotic and biotic stress perception and response*. *Annual Review of Phytopathology*. **52,** 217-594 (2014).

13. Yasuda, M. *et al.* Antagonistic interaction between systemic acquired resistance and the abscisic acid-mediated abiotic stress response in Arabidopsis. *Plant Cell* **20**, 1678–1692 (2008).

14. Zhang, J., Nguyen, H. T. & Blum, A. Genetic analysis of osmotic adjustment in crop plants. *J. Exp. Bot.* **50**, 291–302 (1999).

15. Gechev, T. S., Dinakar, C., Benina, M., Toneva, V. & Bartels, D. Molecular mechanisms of desiccation tolerance in resurrection plants. *Cell. Mol. Life Sci.* **69**, 3175–3186 (2012).

16. Norwood, M., Truesdale, M. R., Richter, A. & Scott, P. Metabolic changes in leaves and roots during dehydration of the resurrection plant Craterostigma plantagineum (Hochst). *South African J. Bot.* **65**, 421–427 (1999).

17. Griffiths, C. A., Gaff, D. F. & Neale, A. D. Drying without senescence in resurrection plants. *Front. Plant Sci.* **5**, 1–18 (2014).

18. Gessler, A., Bottero, A., Marshall, J. & Arend, M. The way back: recovery of trees from drought and its implication for acclimation. *New Phytol.* **228**, 1704–1709 (2020).

19. Hagedorn, F. *et al.* Recovery of trees from drought depends on belowground sink control. *Nat. Plants* **2**, 1-5 (2016).

20. Galiano, L., Martínez-Vilalta, J. & Lloret, F. Carbon reserves and canopy defoliation determine the recovery of Scots pine 4yr after a drought episode. *New Phytol.* **190**, 750–759 (2011).

21. Brodribb, T. J. & Cochard, H. Hydraulic failure defines the recovery and point of death in water-stressed conifers. *Plant Physiol.* **149**, 575–584 (2009).

22. Ingrisch, J. & Bahn, M. Towards a Comparable Quantification of Resilience. *Trends Ecol. Evol.* **33**, 251–259 (2018).

23. Ruehr, N. K., Grote, R., Mayr, S. & Arneth, A. Beyond the extreme: Recovery of carbon and water relations in woody plants following heat and drought stress. *Tree Physiol.* **39**, 1285–1299 (2019).

24. Soma, F., Takahashi, F., Yamaguchi-Shinozaki, K. & Shinozaki, K. Cellular phosphorylation signaling and gene expression in drought stress responses: Aba-dependent and aba-independent regulatory systems. *Plants* **10**, 1–16 (2021).

25. Bhargava, S. & Sawant, K. Drought stress adaptation: Metabolic adjustment and regulation of gene expression. *Plant Breed.* **132**, 21–32 (2013).

bioRxiv preprint doi: https://doi.org/10.1101/2023.02.27.530256; this version posted February 27, 2023. The copyright holder for this preprint (which was not certified by peer review) is the author/funder, who has granted bioRxiv a license to display the preprint in perpetuity. It is made available under a CC-BY-ND 4.0 International license.

26. Oono, Y. *et al.* Monitoring expression profiles of Arabidopsis gene expression during rehydration process after dehydration using ca. 7000 full-length cDNA microarray. *Plant J.* **34**, 868–887 (2003).

27. Huang, D., Wu, W., Abrams, S. R. & Cutler, A. J. The relationship of drought-related gene expression in Arabidopsis thaliana to hormonal and environmental factors. *J. Exp. Bot.* **59**, 2991–3007 (2008).

28. Kim, J. M. *et al.* Transition of chromatin status during the process of recovery from drought stress in arabidopsis thaliana. *Plant Cell Physiol.* **53**, 847–856 (2012).

29. Ding, Y., Fromm, M. & Avramova, Z. Multiple exposures to drought 'train' transcriptional responses in Arabidopsis. *Nat. Commun.* **3**, (2012).

30. Kim, Y. K., Chae, S., Oh, N. I., Nguyen, N. H. & Cheong, J. J. Recurrent Drought Conditions Enhance the Induction of Drought Stress Memory Genes in Glycine max L. *Front. Genet.* **11**, 1–9 (2020).

31. Gonzalez, S., Swift, J., Xu, J., Illouz-eliaz, N. & Nery, J. R. Mimicking genuine drought responses using a high throughput plate assay. Preprint at *BioRxiv, doi: doi.org/10.1101/2022.11.25.517922* (2022).

32. Msanne, J., Lin, J., Stone, J. M. & Awada, T. Characterization of abiotic stress-responsive Arabidopsis thaliana RD29A and RD29B genes and evaluation of transgenes. *Planta* **234**, 97–107 (2011).

33. Aubert, Y. *et al.* RD20, a stress-inducible caleosin, participates in stomatal control, transpiration and drought tolerance in Arabidopsis thaliana. *Plant Cell Physiol.* **51**, 1975–1987 (2010).

34. Székely, G. *et al.* Duplicated P5CS genes of Arabidopsis play distinct roles in stress regulation and developmental control of proline biosynthesis. *Plant J.* **53**, 11–28 (2008).

35. Audenaert, K., De Meyer, G. B. & Höfte, M. M. Abscisic acid determines basal susceptibility of tomato to Botrytis cinerea and suppresses salicylic acid-dependent signaling mechanisms. *Plant Physiol.* **128**, 491–501 (2002).

36. Kawa, D. & Brady, S. M. Root cell types as an interface for biotic interactions. *Trends Plant Sci.* 1–14 (2022).

37. Satija, R., Farrell, J. A., Gennert, D., Schier, A. F. & Regev, A. Spatial reconstruction of single-cell gene expression data. *Nat. Biotechnol.* **33**, 495–502 (2015).

38. Xi, N. M. & Li, J. J. Benchmarking Computational Doublet-Detection Methods for Single-Cell RNA Sequencing Data. *Cell Syst*. **12**, 176-194 (2021).

39. Davière, J.-M. & Achard, P. Gibberellin signaling in plants. *Development*. **140**, 1147–1151 (2013).

40. Bjornson, M., Pimprikar, P., Nürnberger, T. & Zipfel, C. The transcriptional landscape of Arabidopsis thaliana pattern-triggered immunity. *Nat. Plants.* **7**, 579–586 (2021).

41. Lau, J. A. & Lennon, J. T. Rapid responses of soil microorganisms improve plant fitness in novel environments. *Proc. Natl. Acad. Sci. U. S. A*. **109**, 14058–14062 (2012).

42. Mwimba, M. et al. Daily humidity oscillation regulates the circadian clock to influence plant physiology. *Nat. Commun*. **9**, 1–10 (2018).

43. Wang, W. et al. Timing of plant immune responses by a central circadian regulator. *Nature*. **470**,

bioRxiv preprint doi: https://doi.org/10.1101/2023.02.27.530256; this version posted February 27, 2023. The copyright holder for this preprint (which was not certified by peer review) is the author/funder, who has granted bioRxiv a license to display the preprint in perpetuity. It is made available under a CC-BY-ND 4.0 International license.

110–115 (2011).

44. Zhou, M. et al. Redox rhythm reinforces the circadian clock to gate immune response. *Nature*. **523**, 472–476 (2015).

45. Prasanth, M., Ramesh, N., Gothandam, K. M., Sivamangala, K. & Shanthini, T. Pseudomonas Syringae: An Overview and its future as a Rain Making Bacteria. *Int. Res. J. Biol. Sci.* **4**, 70–77 (2015).

46. Schwartz, H. F., Otto, K. L. & Gent, D. H. Relation of temperature and rainfall to development of Xanthomonas and Pantoea leaf blights of onion in Colorado. *Plant Dis.* **87**, 11–14 (2003).

47. Palmero, D. et al. Fungal microbiota from rain water and pathogenicity of Fusarium species isolated from atmospheric dust and rainfall dust. *J. Ind. Microbiol. Biotechnol*. **38**, 13–20 (2011).

48. Xin, X. F. et al. Bacteria establish an aqueous living space in plants crucial for virulence. *Nature*. **539**, 524–529 (2016).

49. Matsumura, M. et al. Mechanosensory trichome cells evoke a mechanical stimuli–induced immune response in Arabidopsis thaliana. *Nat. Commun*. **13**, 1–15 (2022).

50. Sapolsky, R. M., Romero, L. M. & Munck, A. U. How do glucocorticoids influence stress responses? Integrating permissive, suppressive, stimulatory, and preparative actions. *Endocr. Rev.* **21**, 55–89 (2000).

51. Emonet, A. et al. Spatially Restricted Immune Responses Are Required for Maintaining Root Meristematic Activity upon Detection of Bacteria. *Curr. Biol*. **31**, 1012-1028.e7 (2021).

52. Fröschel, C. et al. Plant roots employ cell-layer-specific programs to respond to pathogenic and beneficial microbes. *Cell Host Microbe.* **29**, 299-310 (2021).

53. Rich-Griffin, C. et al. Regulation of cell type-specific immunity networks in 30rabidopsis roots. *Plant Cell.* **32**, 2742–2762 (2020).

54. Zhou, F. et al. Co-incidence of Damage and Microbial Patterns Controls Localized Immune Responses in Roots. *Cell.* **180**, 440-453.e18 (2020).

55. Iyer-Pascuzzi, A. S. et al. Cell Identity Regulators Link Development and Stress Responses in the Arabidopsis Root. *Dev. Cell*. **21**, 770–782 (2011).

56. Sun, J. et al. Activation of symbiosis signaling by arbuscular mycorrhizal fungi in legumes and riceopen. *Plant Cell.* **27**, 823–838 (2015).

57. Rizhsky, L., Liang, H. & Mittler, R. The combined effect of drought stress and heat shock on gene expression in tobacco. *Plant Physiol*. **130**, 1143–1151 (2002).

58. Bartsch, M. et al. Salicylic acid–independent ENHANCED DISEASE SUSCEPTIBILITY1 signaling in Arabidopsis immunity and cell death is regulated by the monooxygenase FMO1 and the nudix hydrolase NUDT7. *Plant Cell* **18**, 1038-1051 (2006).

59. Zhang, Z. et al. A SNARE-protein has opposing functions in penetration resistance and defence signalling pathways. *Plant Journal.* **49**, 302-312 (2007).

60. Dalal, A., Attia, Z. & Moshelion, M. To produce or to survive: How plastic is your crop stress physiology? *Front. Plant Sci.* **8**, 1–8 (2017).

61. Love, M. I., Huber, W. & Anders, S. Moderated estimation of fold change and dispersion for

bioRxiv preprint doi: https://doi.org/10.1101/2023.02.27.530256; this version posted February 27, 2023. The copyright holder for this preprint (which was not certified by peer review) is the author/funder, who has granted bioRxiv a license to display the preprint in perpetuity. It is made available under a CC-BY-ND 4.0 International license.

RNA-seq data with DESeq2. *Genome Biol*. **15**, 1–21 (2014).

62. Liao, Y., Wang, J., Jaehnig, E. J., Shi, Z. & Zhang, B. WebGestalt 2019: gene set analysis toolkit with revamped UIs and APIs. *Nucleic Acids Res*. **47**, 199–205 (2019).

63. O'Malley, R. C. et al. Cistrome and Epicistrome Features Shape the Regulatory DNA Landscape. *Cell.* **165**, 1280–1292 (2016).

64. McLeay, R. C. & Bailey, T. L. Motif Enrichment Analysis: A unified framework and an evaluation on ChIP data. *BMC Bioinformatics.* **11,** 165 (2010).

65. Zheng, G. X. Y. et al. Massively parallel digital transcriptional profiling of single cells. *Nat. Commun*. **8,** 14049 (2017).

66. Hao, Y. et al. Integrated analysis of multimodal single-cell data. *Cell*. **184**, 3573-3587.e29 (2021).

67. Bais, A. S. & Kostka, D. Scds: Computational annotation of doublets in single-cell RNA sequencing data. *Bioinformatics.* **36**, 1150–1158 (2020)